HIGH-RESOLUTION RIDGE BELT MORPHOLOGY AT DYLACHA DORSA. J. A. Balcerski[1], P. K. Byrne[2], [1]NASA Glenn Research Center, 21000 Brookpark Road, Cleveland, OH 44135. (jeffrey.balcerski@nasa.gov), [2]Planetary Research Group, North Carolina State University, Raleigh, NC.

Introduction: Ridge belts on Venus are relatively narrow, positive-relief features that are generally tens of km wide, up to thousands of km in length, and can have hundreds of meters of relief [e.g. 1-3]. These belts often border and delineate expansive, low-lying and relatively featureless plains and are often found in, or grade into, tesserae and dorsae. Geologic interpretations of these belts vary from volcanic construction, to crustal extensional, to collisional underplating. The relative timing of formation of ridge belts does not appear to be confined to a specific chronologic window, nor is there a clear universal relationship between belt formation, local radar-bright lineaments, surrounding terranes, and other regional structures [2].

Morphologic analyses, especially of small-scale features within the belt structure, have been restricted by the relatively low 5 km/px resolution of the Magellan GTDR topography product. Nonetheless, geologic interpretations based upon this data set, and on higher-resolution radar reflectivity products, have produced model chronologies and formation mechanisms for specific study locations. The recent availability of stereo-derived topography for ~20% of the planet at a resolution of 1–2 km/px [4], substantially improved over the GTDR data, provides an opportunity to further investigate the morphologic character of this type of landform on Venus. Specifically, this allows for the differentiation between symmetric and asymmetric ridges, a refinement of the shape of grooves and valleys within the ridge structure and a better understanding of the relationship between radar-bright lineations and the ridge (and surrounding) topography.

Location: We selected a ridge belt that was well-represented in both the Magellan GTDR and improved topographic products (hereafter, the "Herrick et al. models" [4]), as well as the 75 m Magellan FMAP mosaics. This belt links the southern portion of Dylacha Dorsa near 16° S latitude to the northern end of Xi Wang-Mu Tessera around 25° S latitude; the landform has a generally NE strike and spans 66–78° E longitude. This location has not specifically been selected for prior analysis, but it bears characteristics similar to the "broad arch" categorization of an earlier study [2], with an average width around 50 km and length of about 1500 km.

Process: We constructed eight topographic profiles oriented as close to perpendicular to the belt strike as the stereotopo data permitted (Figure 1). These data have resolutions that are highly variable, so we selected profiles from those locations with the highest resolution. The resulting profiles were compared with those over the same sections taken from GTDR data. Using the increased resolution provided by the Herrick et al. models, we compared locations of the radar-bright parallel/subparallel lineations within the belt structure to the topographic expression of the belt. Two well-resolved sample profiles are shown in Figures 2 and 3. These profiles were then inspected for any apparent (a)symmetries in texture or topography.

Observations: A plan-view inspection of the FMAP radar intensities shows that the plains material nearest the ridge is cut by lineations that are oriented approximately parallel to the strike of the ridge. These lineations increase in areal density (i.e., the inter-lineation space decreases) the closer they lie to the highest topographic point on the ridge. In the northern portion (Dylacha Dorsa), the lineations are superposed over the chaotic terrane positioned to the northeast of Nishtigri Corona, but they are no longer apparent as the ridge approaches Xi Wang-Mu Tessera. However, radar-bright fabric remains present in and confined by the ridge belt throughout its entire length. That this fabric of lineations is present only on the southeast side of the ridge leads to our conclusion that it is evidence of shortening strain, consistent with previous assessments [2].

Topographic analysis: Profiles a and b [Figure 2] were obtained with the locally-highest resolution available from the stereotopography product [4]. Whereas data from the GTDR are insufficient to distinguish between a symmetric or asymmetric ridge character, the stereotopo data clearly show that the ridge is composed of asymmetric flanks with multiple peaks and valleys. Profiles c, d, and e (not shown) display similar characteristics, with decreasing ridge elevation in the northern sections. We note that both the asymmetric character and overall magnitude of all profiles are strikingly similar to lunar and martian wrinkle ridges [2, 5-8], thus providing an opportunity for future kinematic and modeling studies [e.g. 9].

Discussion: The increase in resolution provided by stereo-derived topography [4] provides critical context for the striking contrast in radar brightness between the bright lineations that characterize the ridge interior, and the bounding dark, smooth ridges. Prior analysis of radar reflectivity concluded that, in most cases, the surrounding plains material was emplaced after ridge formation, but allowed for exceptions in which the timing was either reversed or ambiguous [4]. We observe that the plains proximal to the northern end of the ridge belt

are cut by the same lineations that run along the ridge strike, thus indicating that at least some portion of the belt formed after plains emplacement [10].

The presence of radar-bright lineations within the belt, but present on both the slopes and valleys therein, suggests that this material existed prior to the deformation event and was incorporated into the belt during its formation. However, the asymmetry of the lineations, being present only on the southeast side of the ridge axis and decreasing in density with distance away from the ridge, leads us to conclude that these lineations are likely small-scale ridges that have been roughened by brittle failure during crustal shortening. Under this interpretation, the lineations are secondary folds situated atop the primary shortening structure. This structural arrangement is similar to terrestrial imbricate fans and suggests crustal shortening via thrusting along a type of décollement. Given the canonically inferred low water content of Venusian crustal materials [e.g. 11] and that the planet's surface is equivalent to a low metamorphic grade environment, it is unlikely that this décollement exists due to volatile pore pressure or weakly consolidated strata. It is more likely that any such detachment corresponds to a low-strength layer thought to exist within the Cytherean lithosphere [e.g. 12].

It is clear that even the 20% coverage of the planet by the Herrick et al. models [4] offers a considerable improvement over previously available topographic data sets for morphologic analysis. We show here that a re-examination of major landforms like ridge belts is both prudent and promising. Moreover, we emphasize that an improvement in topographic products to 250 meters/pixel, via re-processing of existing data [e.g. 13] or obtained via a new Venus mission, would resolve the topographic structure underlying the intra-ridge lineations and thereby substantially advance our understanding of the mechanics that create these and other widespread tectonic landforms on the planet.

References: [1] Barsukov, V. L. et al. (1986). *JGR, 91, D378-398.* [2] Frank, S. L. and Head, J. W. III. (1990). *Earth, Moon, and Planets*, *50/51*, 421-470. [3] McGill, G. E. and Campbell, B. A. (2006). *JGR, 111, E12006*. [4] Herrick, R. R. et al. (2012). *EOS, 93, No. 12,* 125-126. [5] Watters, T. R. (1988) *JGR Solid Earth, v93, B9,* 10236-10254. [6] Golombek, M. P. et al. (1991). *LPSC XXI.* 679-693. [7] Watters, T. R. and Robinson, M. S. (1997). *JGR, v102, E5,* 10889-10903. [8] Golombek, M. P. et al. (2001). *JGR, v106,* 23811-23821. [9] Watters, T. R. (2004). *Icarus, v171,* 284-294. [10] Byrne P. K. et al. (2018) LPS, 49, abstract 1935. [11] Barsukov, V. L. et al. (1980). *LPSC XI*, 765-773. [12] Mikhail, S. and Heap, M. J. (2017). *Phys. Of Earth and Planetary Int., v268,* 18-34. [13] Hensley, S. et al. (2016). *EUSAR XI.*

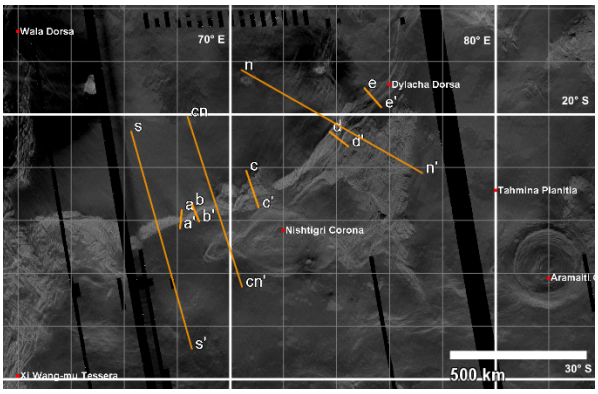

Figure 1. Context image showing local and regional topographic profile overlain on 75m FMAP mosaic. Note that in this image, brightness corresponds to radar reflectivity, not elevation. Ovda Regio lies just off the map to the northeast.

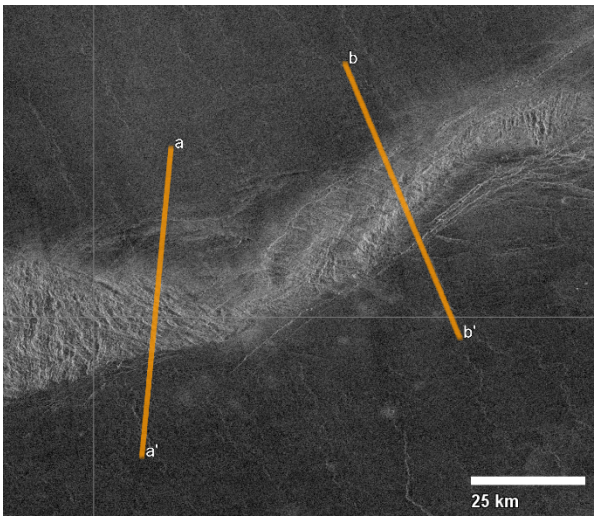

Figure 2. Details of profiles a and b, overlain on 75 m FMAP mosaic basemap.

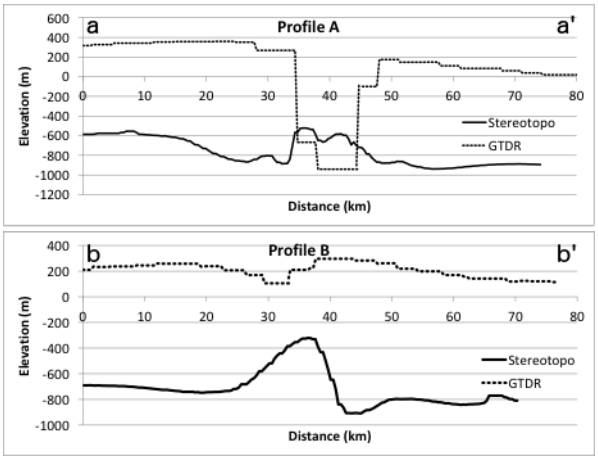

Figure 3. Topographic profiles sections a and b, showing a comparison between Magellan GTDR and sterero-derived topography. Vertical exaggeration = ~25 ×.